

# Prediction of osteoconductive activity of modified potassium fluorrichterite glass-ceramics by immersion in simulated body fluid

Shashwat Bhakta · Deepak K. Pattanayak · Hiroaki Takadama ·  
Tadashi Kokubo · Cheryl A. Miller · Mehdi Mirsaneh · Ian M. Reaney ·  
Ian Brook · Richard van Noort · Paul V. Hatton

Received: 12 November 2009 / Accepted: 3 August 2010 / Published online: 20 August 2010  
© Springer Science+Business Media, LLC 2010

**Abstract** Potassium fluorrichterite ( $\text{KNaCaMg}_5\text{Si}_8\text{O}_{22}\text{F}_2$ ) glass-ceramics were modified by either increasing the concentration of calcium (GC5) or by the addition of  $\text{P}_2\text{O}_5$  (GP2). The stoichiometric composition (GST), GC5 and GP2 were soaked in simulated body fluid (SBF) along with 45S5-type bioglass as a control. After immersion, surface analyses were performed using thin-film X-ray diffraction (TF-XRD), scanning electron microscopy (SEM), energy dispersive X-ray spectroscopy (EDS) and Fourier-transform infrared (reflection) spectroscopy (FT-IR). All compositions showed the formation of a calcium phosphate rich surface layer in SBF; GST, GP2 and the bioglass control within 7 days of immersion and GC5 after 14 days. It was concluded that all compositions were likely to be osteoconductive in vivo, with GP2 providing the best performance in terms of the combination of rapid formation of the surface layer and superior mechanical properties. This glass-ceramic system has potential as a load bearing

bioceramic for fabrication of medical devices intended for skeletal tissue repair.

## 1 Introduction

Surgeons require biocompatible materials that provide consistent clinical results when used to augment or repair bone tissue. Autologous bone is the “gold standard” for these applications, primarily due to its osteoinductive nature and the absence of a hostile immune response in the recipient [1]. Donor site morbidity and the relatively small volume of tissue available are the main limitations associated with autologous bone, and alternatives are therefore used [2]. Bone allograft and xenograft represent alternatives that are frequently used, but demand exceeds supply even though there are widespread concerns regarding the risk of disease transmission. The market for synthetic bone graft substitutes is therefore significant, although existing commercial materials are not ideal. In terms of volume, the main synthetic bone graft substitutes are based on calcium phosphate ceramics (e.g. hydroxyapatite) or bioactive glasses (e.g. 45S5 bioglass). Hydroxyapatite, tricalcium phosphate, and biphasic combinations of the two are the most popular materials used in orthopaedic and craniofacial surgery as simple space fillers and coatings on metal implants. Unfortunately these ceramics are brittle, making them unsuitable for load bearing applications [3]. Bioactive glasses were first developed in 1969 [4] and provided a method of interfacial bonding of an implant with host tissue. The most widely reported composition, 45S5 bioglass, has the ability to form an apatite layer on its surface which is the basis for its bone bonding ability [4]. Like the calcium phosphates, the poor mechanical properties of 45S5 bioglass make it unsuitable for load bearing applications [4].

---

S. Bhakta (✉) · C. A. Miller · I. Brook · R. van Noort ·  
P. V. Hatton  
Centre for Biomaterials and Tissue Engineering,  
School of Clinical Dentistry, University of Sheffield,  
Claremont Crescent, Sheffield S10 2TA, UK  
e-mail: Shashwat.bhakta@sth.nhs.uk

D. K. Pattanayak · H. Takadama · T. Kokubo  
Department of Biomedical Sciences, College of Life and Health  
Sciences, Chubu University, 1200 Matsumoto, Kasugai,  
Aichi 487-8501, Japan

M. Mirsaneh · I. M. Reaney  
Department of Engineering Materials,  
Sir Robert Hadfield Building, University of Sheffield,  
Mappin Street, Sheffield S1 3JD, UK

To summarise, the most commonly used alloplastic bone substitutes have limitations that render them unsuitable for load bearing applications in the skeleton. There remains a demand for a biocompatible and osteoconductive biomaterial that has appropriate mechanical properties. Glass ceramics represent a class of biomaterial that could potentially meet these requirements. Apatite-wollastonite (A-W) glass-ceramic has high fracture toughness  $> 2\text{MPam}^{1/2}$  and bend strength  $> 200\text{ MPa}$  [5]. Commercial manufacture of A-W is however, complex due to surface nucleation of the strengthening wollastonite phase [5, 6]. As a result, A-W glasses cannot be cast directly to net-shape and it is difficult to cost-effectively produce complex or custom prostheses. Alternatives have been investigated, but none have yet proved ideal for commercial adoption. For example, apatite-mullite glass ceramics have relatively high mechanical strength, are castable and volume nucleate [7] but it is postulated that their high alumina content may suppress bioactivity via inhibition of apatite deposition [8, 9].

Glass-ceramics based on chain silicates may offer greater promise as they appear to satisfy most of the criteria for an ideal bioceramic for bone repair. Compositions based on apatite-canasite have been shown to be osteoconductive in vitro [10] and in vivo [11]. Other chain silicates based on potassium fluorrichterite ( $\text{KNaCaMg}_5\text{Si}_8\text{O}_{22}\text{F}_2$ ) also have potential as a bone substitute material capable of withstanding functional loads [12, 13]. These materials have high flexural strengths ( $\sim 250\text{ MPa}$ ) and fracture toughness ( $\sim 2.7\text{ MPam}^{1/2}$ ) [12–15] they bulk nucleate and have a relatively low liquidus temperature, which permits casting to net shape [14, 15]. The phase evolution and structure–property relationships have been extensively characterized [14, 15]. However, they have not been investigated for use as biomaterials to date. The aim of this study was therefore to investigate potassium fluorrichterite compositions that were modified by substitution of 5% CaO for MgO, and by the addition of  $\text{P}_2\text{O}_5$  to the stoichiometric composition, to increase the osteoconductivity as reported in apatite-canasite

glass-ceramics. The osteoconductive potential was determined using immersion in simulated body fluid (SBF) in vitro, a method widely reported as a good predictor of osteoconductivity [16, 17].

## 2 Experimental procedure

### 2.1 Glass preparation

Three glass-ceramic compositions based on potassium fluorrichterite ( $\text{KNaCaMg}_5\text{Si}_8\text{O}_{22}\text{F}_2$ ) were produced: stoichiometric (termed GST), GST with 5 mol% CaO substituted for MgO (termed GC5) and GST with 2 mol%  $\text{P}_2\text{O}_5$  added (termed GP2). Further addition of  $\text{P}_2\text{O}_5$  to GST has been reported to result in severe liquid–liquid phase separation and very poor mechanical properties [18] and therefore was not studied in this work. 45S5-type bioglass [4] was used as a control material. Glass batches were prepared using silica (Loch Aline sand 99.5%  $\text{SiO}_2$ ) and reagent grade chemicals ( $\text{Na}_2\text{CO}_3$ ,  $\text{K}_2\text{CO}_3$ ,  $\text{Mg}(\text{OH})_2$ ,  $\text{CaF}_2$  and  $\text{MgHPO}_4 \cdot 3\text{H}_2\text{O}$ —Fisher Scientific and Sigma-Aldrich). The chemical compositions in mol% are listed below (Table 1).

The glasses were melted in uncovered platinum (with 2% rhodium) crucibles at  $1,400^\circ\text{C}$  ( $1,300^\circ\text{C}$  for bioglass) for 3 h in an electric furnace and stirred for the final 2 h with a platinum stirrer at 60 rpm. All compositions were cast as glass onto a pre-heated steel plate, annealed in a muffle furnace between  $520$  and  $580^\circ\text{C}$  and cooled to room temperature at  $1^\circ\text{C}/\text{min}$ .

As-cast glass was core drilled (Sealey Power Products, Sealey Group, Bury St. Edmunds, UK) using a diamond core drill (HABIT core drill, 12 mm internal diameter, 1 mm thickness, Abrasive Technology Ltd, London, UK) to produce glass cylinders. These were cut using a diamond blade (Diamond wafering blade 15 HC, Buehler, USA) into discs ( $12 \times 2\text{ mm}$ ). To crystallise the glass ceramic specimen, the discs were cerammed for 4 h in a muffle furnace

**Table 1** Chemical composition of GST, GC5, GP2 and bioglass in mol%

Code	$\text{SiO}_2$	$\text{Na}_2\text{O}$	$\text{K}_2\text{O}$	MgO	$\text{CaF}_2$	CaO	$\text{P}_2\text{O}_5$
GST							
Stoichiometric	53.37	3.33	3.33	33.35	6.62	–	–
GC5							
5 mol% CaO subs. for MgO in GST	53.37	3.33	3.33	28.35	6.62	5	–
GP2							
2 mol% $\text{P}_2\text{O}_5$ added to GST	52.26	3.26	3.26	32.66	6.56	–	2
Bioglass							
45S5-type bioglass	45	24.5	–	–	–	24.5	6

(Eurotherm 818 Programmable Furnace, Lenton Thermal Design, Hope Valley, Derbyshire, UK) rising at 5°C/min to 950°C for GST and 1,000°C for GC5 and GP2 and cooled at 5°C/min to room temperature. The discs were finally polished using silicon carbide paper (Buehler-Met II, Buehler UK Ltd, Coventry, UK) of sequentially decreasing coarseness to a P1200 grit surface finish.

## 2.2 Soaking in SBF

Prior to immersion in SBF, discs were cleaned initially with running tap water and then in acetone and ultrapure water (Aquarius water distillation apparatus, RFD250NB, Advantec, Taito-Ku, Tokyo, Japan) in an ultrasonic bath (Branson 1510, Yamato, Tokyo, Japan) for 10 min in each solution. SBF was prepared using the recipe recommended

by Kokubo et al. [19]. The volume of SBF per specimen was calculated using the formula,

$$V_s = S_a/10$$

where,  $V_s$  is the volume of SBF and  $S_a$  is the surface area per disc. SBF (23 ml) was filtered (Minisart, 0.2µm, Sartorius Mechatronics, Japan K.K., Tokyo) and then pipetted into screw top plastic containers with a conical base. Each disc was carefully placed horizontally at the bottom of each container and the under surface was examined for apatite deposition. All discs were handled using metallic tweezers, which were wiped clean with ethanol between each specimen. The containers were placed in an incubator (Eyela NDO-400, Eyela Rikakkai Co. Ltd, Japan) maintained at 36.5°C. All compositions were immersed for 1, 7, 14 and 28 days. On removal from

**Fig. 1** Thin-film XRD (TF-XRD) traces of 45S5-type bioglass before soaking (day 0) and after soaking for 1 and 7 days in SBF

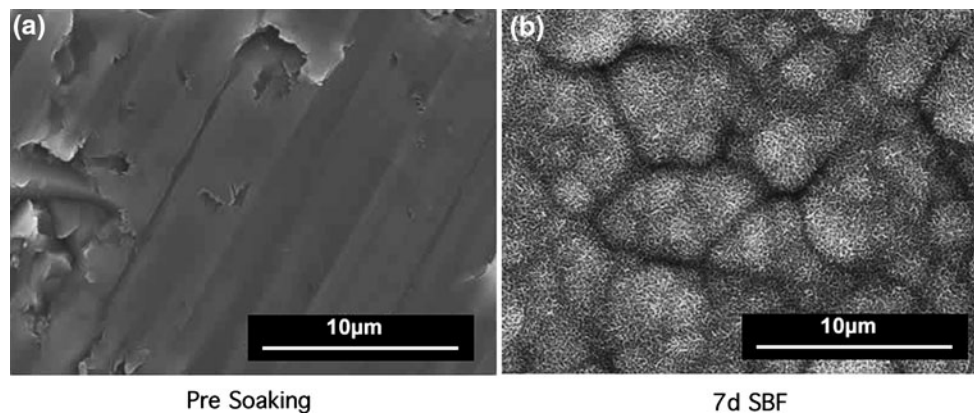
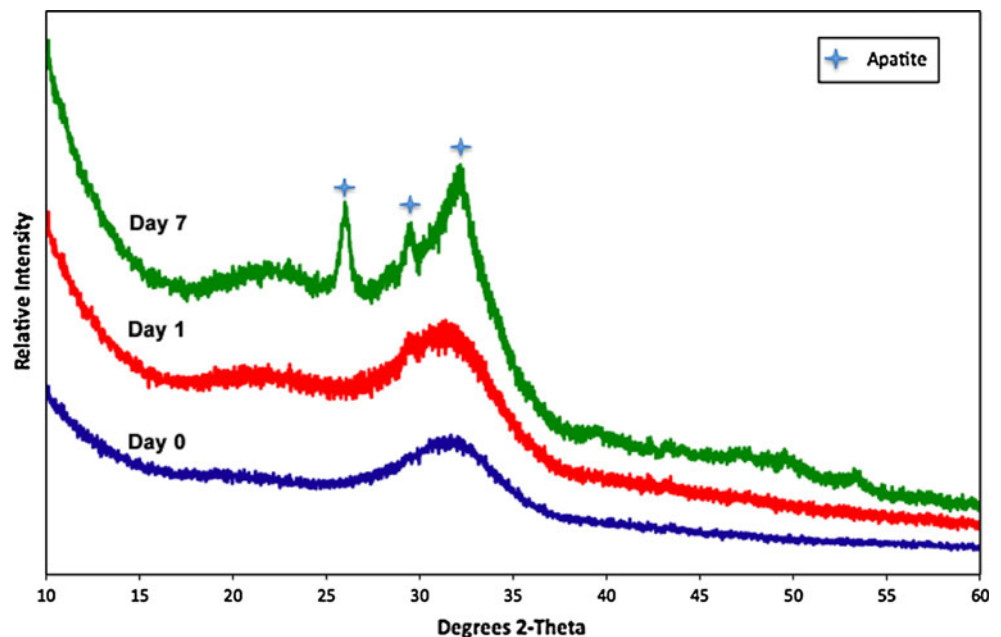


**Fig. 2** FE-SEM images of 45S5-type bioglass before (a) and after 7 days of immersion in SBF (b)

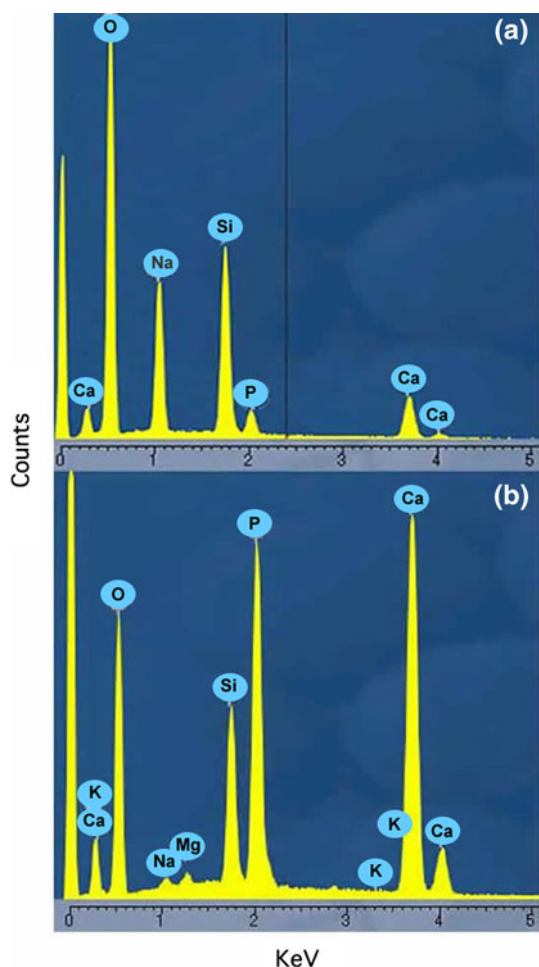
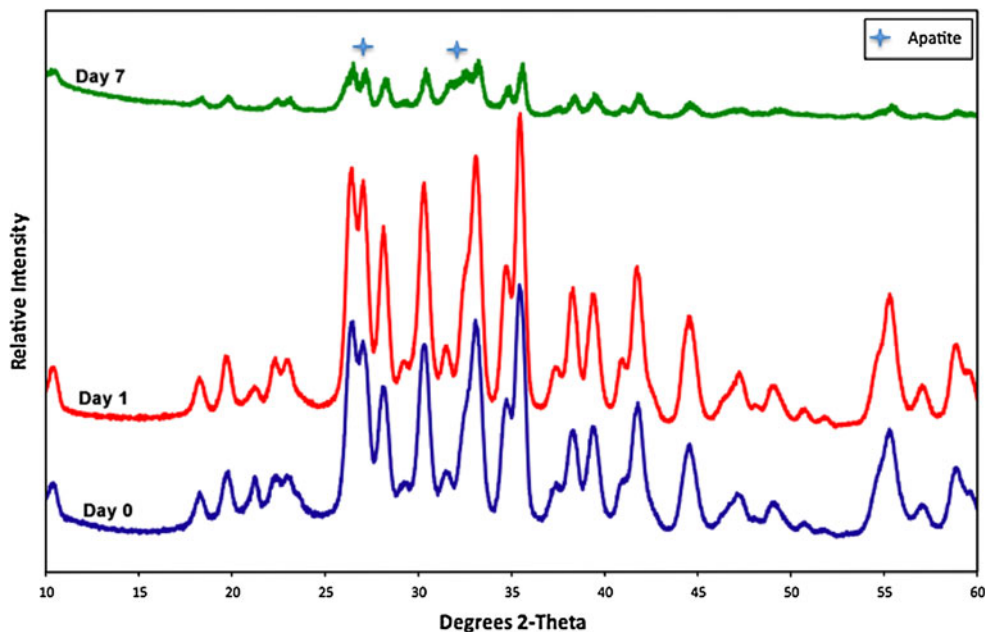


**Fig. 3** EDS spectra from the surface of 45S5-type bioglass before soaking (a) and after 7 days immersion in SBF (b)

**Fig. 4** Thin-film XRD (TF-XRD) traces of GST before soaking (day 0) and after soaking for varying periods in SBF



SBF, discs were rinsed using ultrapure water, placed in plastic storage containers and then dried at 40°C in an incubator for at least 24 h before inspection.

### 2.3 Surface analysis of glasses

Apatite deposition was investigated using thin-film X-ray diffraction (TF-XRD) (Rigaku RINT 2500, Rigaku Corp., Tokyo, Japan) with a scan range from 10 to 60° 2 $\theta$  with a step size of 0.02° using a Cu K $\alpha$  ( $\lambda = 0.15405$  nm) radiation source at a rate of 1°/min with a glancing angle of 1° against the incident beam on the specimen surface. The specimens were placed on a rotating base (rotating at 30 rpm) during measurement. The elemental composition of the specimen surfaces was characterized using energy dispersive X-ray spectroscopy (EDS) (Horiba EMAX, Horiba Ltd., Kyoto, Japan) at 15 kV. FT-IR spectra were obtained from 2,000 to 400 cm $^{-1}$  using JASCO FT/IR 6100 (JASCO Corp, Tokyo, Japan) using the PR-510i accessory at 55°. Following this, the samples were lightly coated with platinum-palladium (E-1030 ion sputter, Hitachi Ltd, Japan) and observed using a field-emission scanning electron microscope (FE-SEM) (Hitachi F-4300, Hitachi Ltd, Japan) operated at 15 kV at a working distance of 15 mm.

## 3 Results and discussion

TF-XRD, EDS and FE-SEM confirmed that 45S5-type bioglass, which was used as a positive control exhibited



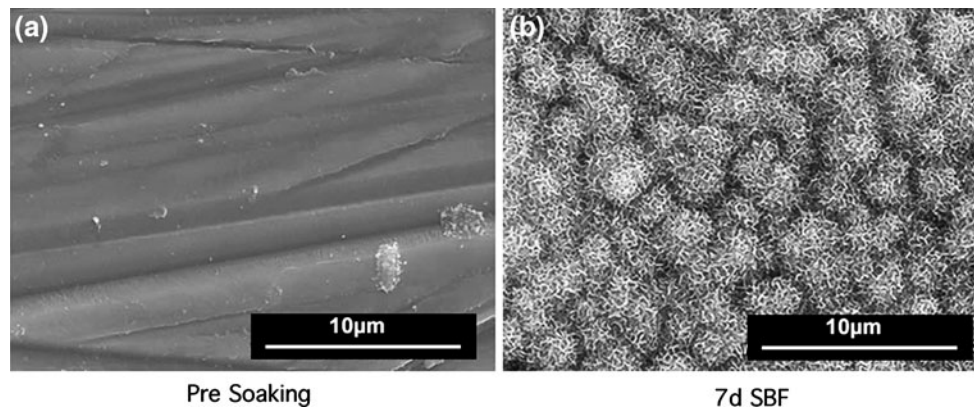


**Fig. 5** FE-SEM images of GST before (a) and after 7 days of immersion in SBF (b)

apatite deposition within 7 days of immersion in SBF. The distinctive peaks at  $26^\circ$ ,  $29^\circ$  and  $32^\circ$   $2\theta$  in TF-XRD plots (Fig. 1) obtained from the surface of 45S5 bioglass after 7 days soaking are strongly indicative of formation of a calcium phosphate surface layer (JCPDS No. 09-0432, Hydroxylapatite).

SEM micrographs taken from the surface of 45S5-type bioglass before (Fig. 2a) and after soaking for 7 days in SBF (Fig. 2b) shows characteristic dome shaped crystals of a calcium phosphate layer on the surface after soaking, which suggests bone-like apatite deposition and therefore potential osteoconductivity [18]. Comparison of EDS spectra taken from the surfaces of the unsoaked (Fig. 3a) and soaked (Fig. 3b) surfaces reveal Ca and P peaks of significantly greater intensity that appear after soaking in SBF. This change in the EDS spectrum can be interpreted as further evidence of the formation of a surface calcium phosphate layer. The Ca:P ratio of the surface layer was obtained as 1.708, which could be interpreted as hydroxyapatite [20]. The bioactivity of 45S5-type bioglass is known to arise from the formation of a silica rich surface layer, which permits ion exchange between the glass and the surrounding environment [16].

Stoichiometric potassium fluorrichterite (GST) is relatively inert, exhibits low solubility and does not significantly leach ions into solution [21]. Moreover, the phase assemblage after suitable heat treatment does not contain any residual glass phase detectable by XRD and conventional electron microscopy [14, 15]. Therefore, this composition was not initially considered to have bioactive potential. The TF-XRD traces for GST before soaking (day 0) and also after 1 and 7 days immersion in SBF are shown in Fig. 4. The complex diffraction trace of the underlying potassium fluorrichterite (KFR) phase within the test composition masks the appearance of new peaks, making the detection of new peaks in the region of  $26^\circ$  and  $32^\circ$   $2\theta$  difficult. However, the attenuation of overall peak intensities on the day 7 trace

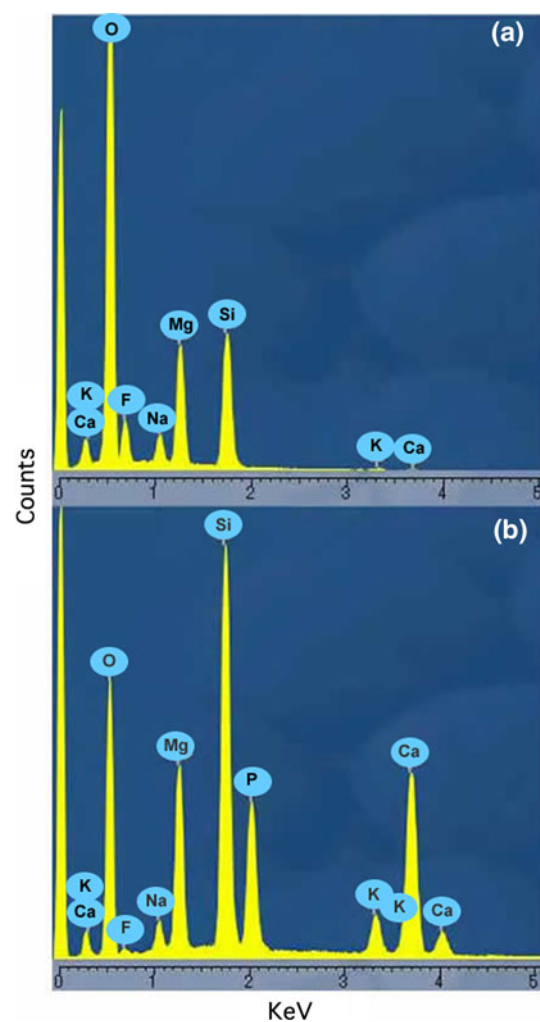


**Fig. 6** EDS spectra from the surface of GST before soaking (a) and after 7 days immersion in SBF (b)

and subtle alterations in this trace, suggestive of new peaks in the region of  $26^\circ$  and  $32^\circ$   $2\theta$ , could be interpreted as evidence of formation of a surface calcium phosphate layer.

**Fig. 7** FT-IR spectra obtained from the surface of GST before soaking (day 0) and following 1 and 7 days of immersion in SBF

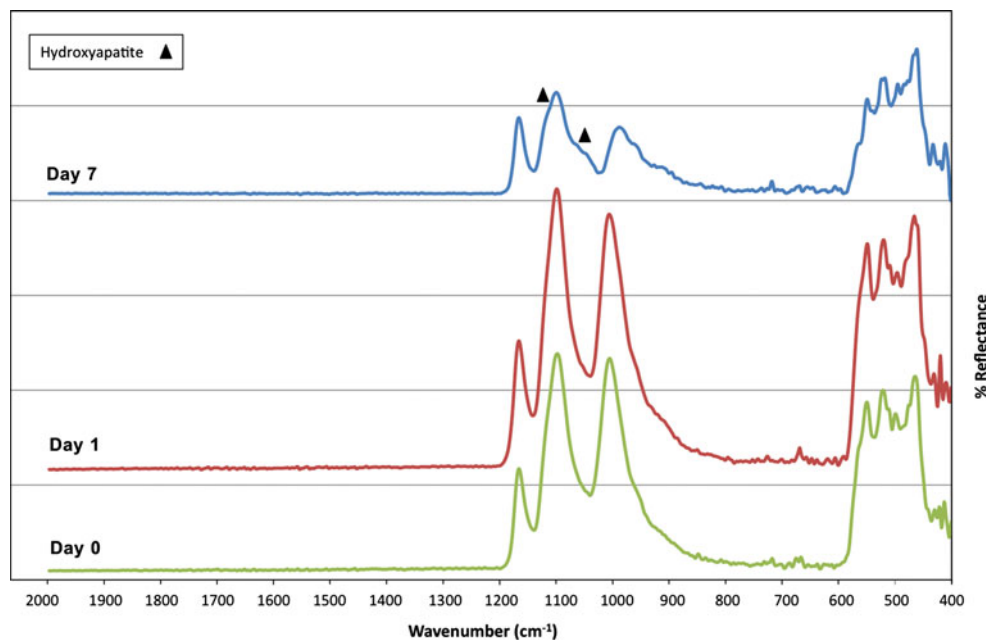


**Fig. 8** Thin-film XRD (TF-XRD) traces of GP2 before soaking (day 0) and after soaking for varying periods in SBF

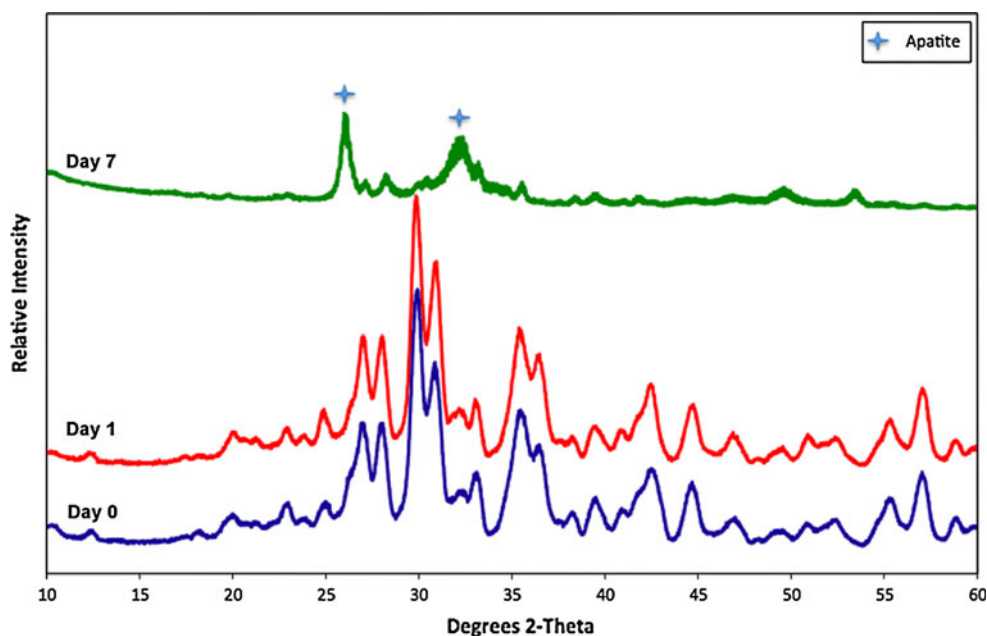
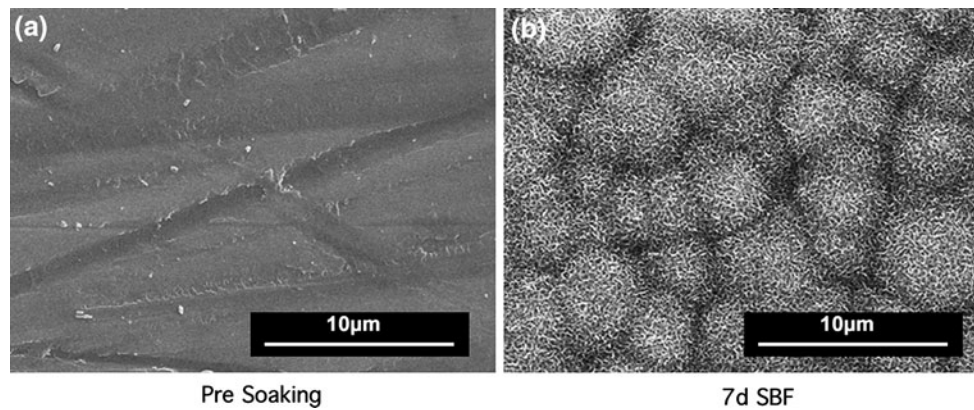


Figure 5 shows FE-SEM micrographs taken of the surface of GST before soaking (a), and following 7 days of immersion in SBF (b). Figure 5b shows the formation of dome shaped apatite crystals. Comparison of the EDS spectra obtained from the surface of GST before (Fig. 6a) and after soaking in SBF (Fig. 6b) shows the formation of distinct Ca and P peaks following soaking, which can be attributed to formation of a surface apatite layer. From the EDS data, the Ca:P ratio obtained was 1.699 for the day 7

sample, which could be interpreted as hydroxyapatite [20]. Figure 7 shows the FT-IR spectra obtained from the surface of GST before immersion and following 1 and 7 days in SBF. The appearance of two new peaks at approximately  $1,050$  and  $1,120\text{ cm}^{-1}$  are suggestive of the formation of apatite [10, 16].

GP2 was modified from the stoichiometric composition by the addition of 2 mol%  $\text{P}_2\text{O}_5$ . The TF-XRD traces detected the formation of new crystalline peaks in the



**Fig. 9** FE-SEM images of GP2 before (a) and after 7 days of immersion in SBF (b)

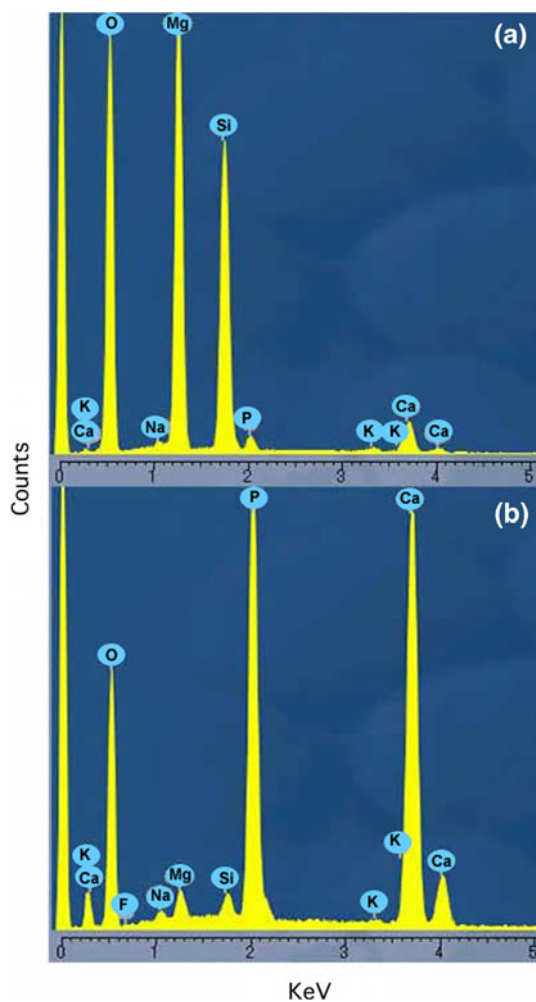


**Fig. 10** EDS spectra from the surface of GP2 before soaking (a) and after 7 days immersion in SBF (b)

region of  $26^\circ$  and  $32^\circ$   $2\theta$ , along with attenuation in the intensity of the underlying crystalline KFR peaks, suggestive of the deposition of a thick calcium phosphate

surface layer (Fig. 8). The presence of this layer was confirmed by FE-SEM (Fig. 9), which showed dome-shaped crystals suggestive of the formation of bone-like apatite and by EDS (Fig. 10), which showed a significant increase in the intensity of Ca and P peaks following soaking in SBF. From the EDS data, the Ca:P ratio obtained for the day 7 sample was 1.519. Further analysis of the day 14 and day 28 samples resulted in Ca:P ratios of 1.579 and 1.585 respectively. Though EDS provides some insight into the nature of new mineral layers formed by interaction of a ceramic with SBF, it is also well-known that data from EDS in the SEM is influenced by a number of factors including detector sensitivity (and relative differences in sensitivity to different elements), specimen geometry/topography, surface layer thickness, and analysis conditions (e.g. accelerating voltage). EDS data should be viewed in the context of these limitations, and not be subjected to “over interpretation”. However, one possible explanation is that the surface calcium phosphate layer is thinner than the penetration depth of the X-rays, therefore the EDS data obtained may have higher levels of phosphate due to the greater concentration of  $P_2O_5$  within GP2, which in turn affects the Ca:P ratio. FT-IR spectra obtained from the surface of GP2 (Fig. 11) shows the formation of new peaks in the region of  $570$ ,  $1050$  and  $1120\text{ cm}^{-1}$ , which are suggestive of the formation of hydroxyapatite [10, 16].

It is generally believed that for a glass to be bioactive in SBF, a silica rich layer capable of ion exchange must first form on the surface of the material, Ca and P then react to form amorphous apatite on this Si rich layer that eventually crystallizes into hydroxyapatite [4]. Therefore, the presence of soluble  $SiO_2$  in a glass ceramic is considered to be crucial for osteoconductivity. The exception to this model is where an apatite phase is already present in the biomaterial, which can lead to Ca and P precipitating directly on the surface without the formation of a Si rich layer [22].

**Fig. 11** FT-IR spectra obtained from the surface of GP2 before soaking (day 0) and following 1 and 7 days of immersion in SBF

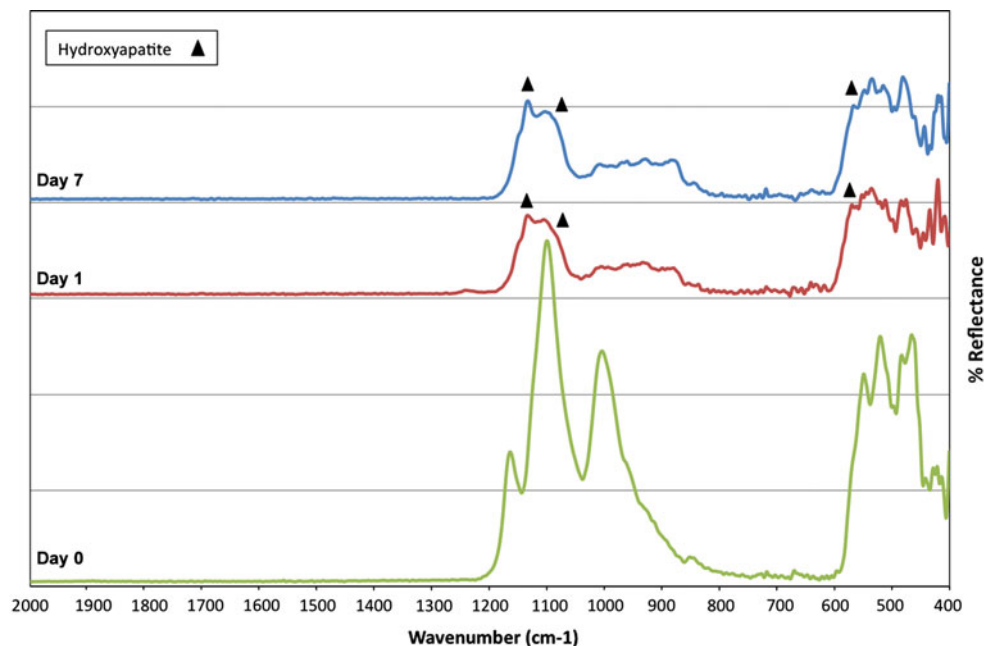
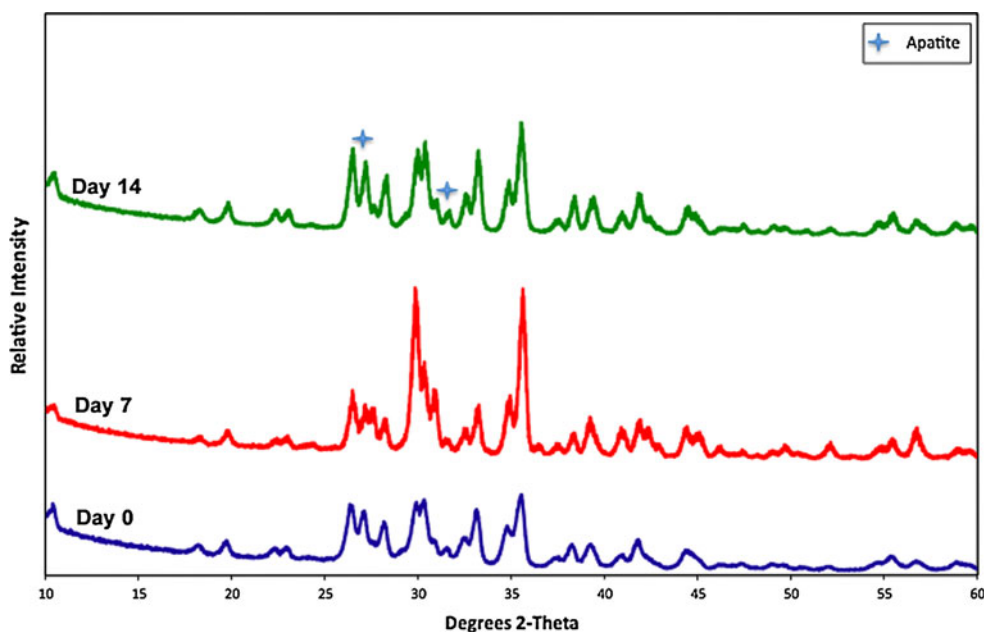


**Fig. 12** Thin-film XRD (TF-XRD) traces of GC5 before soaking (day 0) and after soaking for varying periods in SBF



Therefore, the bioactivity exhibited by GP2 may either be due to its crystalline phase, which contains fluorapatite [12–14] or the residual glass phase, which is Si rich [13, 14].

Although GC5 did not form a calcium phosphate surface layer within 7 days, there was evidence of such a layer by day 14. Similar to GST, the TF-XRD results (Fig. 12) were difficult to interpret. However, the presence of the calcium phosphate surface layer at day 14 was confirmed by

FE-SEM (Fig. 13), which, in spite of showing a slightly different surface microstructure, still exhibited the formation of a thick surface layer with clearly distinguishable dome-shaped crystals of bone-like apatite. EDS (Fig. 14) showed an increase in the intensity of Ca and P peaks, which could be attributed to the surface layer. From the EDS data, the Ca:P ratio obtained for the day 7 sample was 17.148. It is important to consider that the day 7 sample did not show the formation of a surface layer. Further analysis



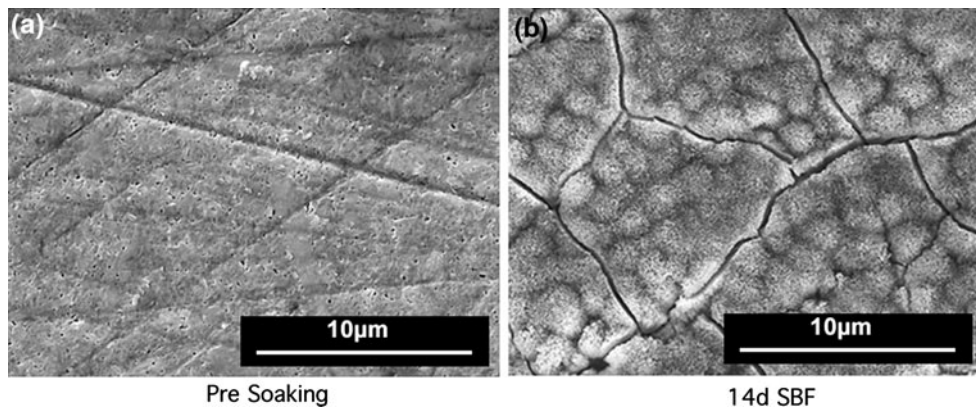


**Fig. 13** FE-SEM images of GC5 before (a) and after 14 days of immersion in SBF (b)

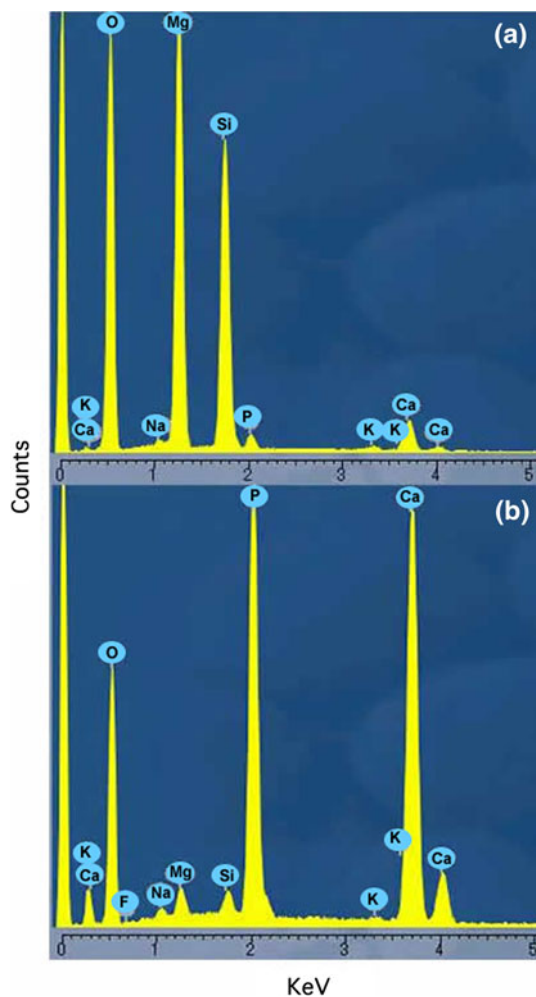


**Fig. 14** EDS spectra from the surface of GC5 before soaking (a) and after 14 days in SBF (b)

of the day 14 and day 28 samples resulted in Ca:P ratios that dropped to 2.461 for the day 14 sample and to 1.733 for the day 28 sample. Taking the limitations of EDS into

account, as discussed earlier, one possible explanation could be the high Ca level within GC5 affecting the Ca:P ratio. FT-IR spectra obtained from the surface of GC5 (Fig. 15), showed the formation of new peaks in the region of 570, 1050 and 1120  $\text{cm}^{-1}$ , indicative of the formation of hydroxyapatite [10, 16].

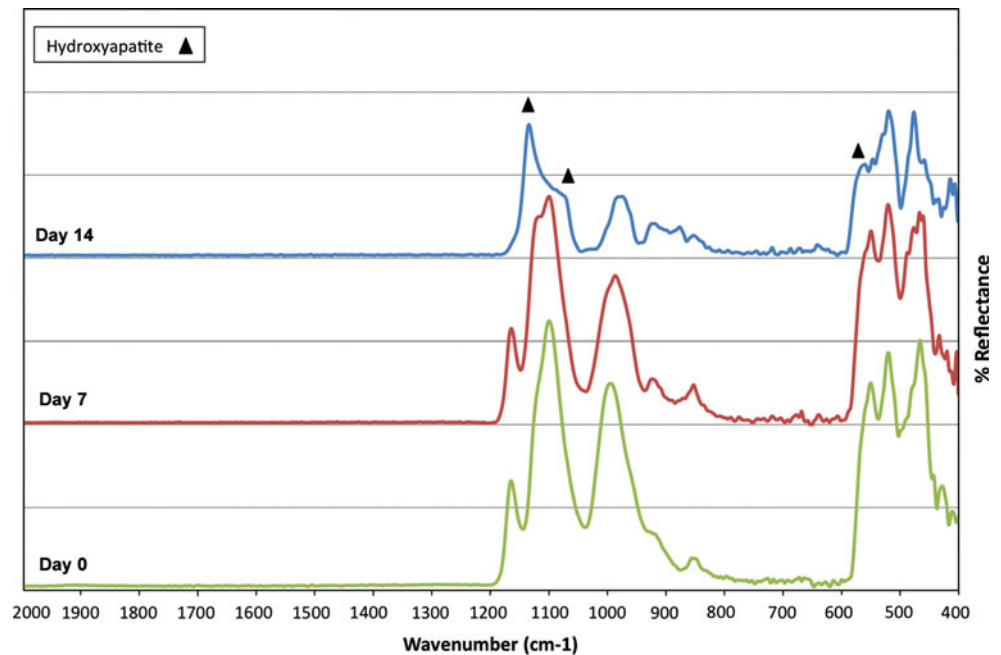
The formation of this surface layer after 14 days immersion indicates that GC5 is also potentially osteoconductive but perhaps at a slower rate as compared to GP2 and GST.

Two mechanisms could account for predicted bioactivity in these systems. One involves the reactivity of a residual glass phase capable of ion exchange while the other is related to the presence of a surface apatite phase that facilitates nucleation and crystal growth. Unfortunately it is not possible to discriminate between them with a high degree of certainty. Given the relatively small quantity of residual glass in these systems, it seems likely that it is the latter that is dominating here. This suggestion is supported by a recently published study of the response of bone tissue to modified fluorocanite glass-ceramic [23].

#### 4 Conclusions

The potassium fluorrichterite (KFR) compositions evaluated in this study: stoichiometric (GST), GP2 (2 mol%  $\text{P}_2\text{O}_5$  added to GST) and GC5 (5 mol% CaO substituted for MgO in GST) all demonstrated apatite deposition following immersion in SBF and are therefore represent a potentially osteoconductive bioceramic system. Potassium fluorrichterite is therefore likely to be useful as a load bearing glass-ceramic for fabrication of medical devices intended for skeletal tissue repair, with GP2 showing the greatest promise based on its mechanical properties [14] and osteoconductive potential.

**Fig. 15** FT-IR spectra obtained from the surface of GC5 before soaking (day 0) and following 7 and 14 days immersion in SBF



## References

- Moreau JL, Caccamese JF, Coletti DP, Sauk JJ, Fisher JP. Tissue engineering solutions for cleft palates. *J Oral Maxillofac Surg.* 2007;65(12):2503–11.
- Parikh SN. Bone graft substitutes: past, present, future. *J Postgrad Med.* 2002;48(2):142–8.
- Akao M, Aoki H, Kato K. Mechanical properties of sintered hydroxyapatite for prosthetic applications. *J Mater Sci.* 1981; 16(3):809–12.
- Hench LL. The story of bioglass. *J Mater Sci Mater Med.* 2006;17(11):967–78.
- Kokubo T, Shigematsu M, Nagashima Y, Tashiro M, Nakamura T, Yamamuro T, Higashi S. Apatite and wollastonite containing glass-ceramics for prosthetic applications. *Bull Inst Chem Res Kyoto Univ.* 1982;60:260–8.
- Kokubo T. A-W glass-ceramics: processing and properties. In: Hench LL, Wilson J, editors. *An introduction to bioceramics.* Singapore: World Scientific; 1993. p. 75–88.
- Hill R, Wood D. Apatite-mullite glass-ceramics. *J Mater Sci Mater Med.* 1995;6:311–8.
- Ohtsuki C, Kokubo T, Yamamuro T. Compositional dependence of bioactivity of glasses in the system CaO–SiO<sub>2</sub>–Al<sub>2</sub>O<sub>3</sub>; its in vitro evaluation. *J Mater Sci Mater Med.* 1992;3:119–25.
- Ohura KNT, Yamamuro T, Ebisawa Y, Kokubo T, Kotoura Y, Oka M. Bioactivity of CaO.SiO<sub>2</sub> glasses added with various ions. *J Mater Sci Mater Med.* 1992;3:95–100.
- Miller CA, Kokubo T, Reaney IM, Hatton PV, James PF. Formation of apatite layers on modified canasite glass-ceramics in simulated body fluid. *J Biomed Mater Res.* 2001;59(3):473–80.
- Freeman CO BI, Johnson A, Hatton PV, Hill RG, Stanton KT. Crystallization modifies osteoconductivity in an apatite-mullite glass-ceramic. *J Mater Sci Mater Med.* 2003;14(11):985–90.
- Beall GH, Meagles JE Jr. Potassium fluorrichterite glass ceramics and method. US Patent 4467039, 1984.
- Beall GH. Chain silicate glass-ceramics. *J Non-Cryst Solids.* 1991;129:163–73.
- Mirsaneh M, Reaney IM, Hatton PV, James PF. Characterization of high-fracture toughness K-fluorrichterite-fluorapatite glass ceramics. *J Am Ceram Soc.* 2004;87(2):240–6.
- Mirsaneh M, Reaney IM, James PF, Hatton PV. Effect of CaF<sub>2</sub> and CaO substituted for MgO on the phase evolution and mechanical properties of K-fluorrichterite glass ceramics. *J Am Ceram Soc.* 2006;89(2):587–95.
- Hench LL. Bioceramics: from concept to clinic. *J Am Ceram Soc.* 1991;74(7):1487–510.
- Kokubo T, Kushitani H, Sakka S, Kitsugi T, Yamamuro T. Solutions able to reproduce in vivo surface structures changes in bioactive glass-ceramic A-W. *J Biomed Mater Res.* 1990;24: 721–34.
- Mirsaneh M, Reaney IM, James PF, Bhakta S, Hatton PV. Effect of P<sub>2</sub>O<sub>5</sub> on the early stage crystallisation of potassium fluorrichterite. *J Non-Cryst Solids.* 2008;354(28):3362–8.
- Kokubo T, Takadama H. How useful is SBF in predicting in vivo bone bioactivity? *Biomaterials.* 2006;27(15):2907–15.
- Benhayoune H, Charlier D, Jallot E, Laquerriere G, Balossier G, Bonhomme P. Evaluation of the Ca/P concentration ratio in hydroxyapatite by STEM-EDXS: influence of the electron irradiation dose and temperature processing. *J Phys D Appl Phys.* 2001;34:141–7.
- Bhakta S, Hurrell-Gillingham K, Mirsaneh M, Miller CA, Reaney IM, Brook IM, van Noort R, Hatton PV. Biocompatibility of modified fluorrichterite glass-ceramic compositions. Submitted to *J Mater Sci Mater Med.*
- Kokubo T. Surface chemistry of bioactive glass-ceramics. *J Non-Cryst Solids.* 1990;120:138–51.
- Bandyopadhyay-Ghosh S, Faria PEP, Johnson A, Felipucci DNB, Reaney IM, Salata LA, Brook IM, Hatton PV. Osteoconductivity of modified fluorocanase glass-ceramics for bone tissue augmentation and repair. *J Biomed Mater Res A.* 2010;94A:760–8